Atmos. Chem. Phys. Discuss., 9, 26095–26142, 2009
www.atmos-chem-phys-discuss.net/9/26095/2009/

Atmospheric Chemistry and Physics Discussions

This discussion paper is/has been under review for the journal Atmospheric Chemistry and Physics (ACP). Please refer to the corresponding final paper in ACP if available.

A multi-model analysis of vertical ozone profiles

J. E. Jonson[1], A. Stohl[2], A. M. Fiore[3], P. Hess[4], S. Szopa[5], O. Wild[6], G. Zeng[7,*], F. J. Dentener[8], A. Lupu[9], M. G. Schultz[10], B. N. Duncan[11], K. Sudo[12], P. Wind[1], M. Schulz[5], E. Marmer[8], C. Cuvelier[8], T. Keating[13], A. Zuber[14], A. Valdebenito[1], V. Dorokhov[15], H. De Backer[16], J. Davies[17], G. H. Chen[18], B. Johnson[19], and D. W. Tarasick[17]

[1]Norwegian Meteorological Institute, Oslo, Norway
[2]NILU, Kjeller, Norway
[3]Geophysical Fluid Dynamics Laboratory, NOAA, Princeton, NJ, USA
[4]National Center for Atmospheric Research, Boulder, CO, USA
[5]Laboratoire des Sciences du Climat et de l'Environnement, CEA/CNRS/UVSQ/IPSL, Gif-sur-Yvette, France
[6]Lancaster Environment Centre, Lancaster University, Lancaster, UK
[7]Centre for Atmospheric Science, University of Cambridge, Cambridge, UK
[8]European Commission, DG-Joint Research Centre, Institute for Environment and Sustainability, Ispra, Italy
[9]Center for research in Earth and Space Science, York University, York, Canada
[10]ICG-2, Forchungszentrum-Jülich, Jülich, Germany

[11]NASA Goddard Space Flight Center, Baltimore, MD, USA
[12]Grad. School of Environ. Studies, Nagoya University, Nagoya, Japan
[13]Office of Policy Analysis and Review, Environmental Protection Agency, Washington DC, USA
[14]Environment Directorate General, European Commission, Brussels, Belgium
[15]Central Aerological Observatory, Moscow, Russia
[16]Royal Meteorological Institute of Belgium (R. M. I. B.), Brussels, Belgium
[17]Environmental Canada, Downsview, Canada
[18]Central Weather Bureau, Taipei, Taiwan
[19]NOAA/ESRL, Boulder, CO, USA
[*]now at: National Institute of Water and Atmospheric Research, Lauder, New Zealand

Received: 14 October 2009 – Accepted: 27 November 2009 – Published: 8 December 2009

Correspondence to: J. E. Jonson (j.e.jonson@met.no)

Published by Copernicus Publications on behalf of the European Geosciences Union.

Abstract

A multi-model study of the long-range transport of ozone and its precursors from major anthropogenic source regions was coordinated by the Task Force on Hemispheric Transport of Air Pollution (TF HTAP) under the Convention on Long-range Transboundary Air Pollution (LRTAP). Vertical profiles of ozone at 12-h intervals in year 2001 are available from twelve of the models contributing to this study and are compared here with observed profiles from ozonesondes. The contributions from each major source region are analysed for selected sondes, and this analysis is supplemented by retroplume calculations using the FLEXPART Lagrangian particle dispersion model to provide insight into the origin of ozone transport events and the cause of differences between the models and observations.

In the boundary layer ozone levels are in general strongly affected by regional sources and sinks. With a considerably longer lifetime in the free troposphere, ozone here is to a much larger extent affected by processes on a larger scale such as intercontinental transport and exchange with the stratosphere. Such individual events are difficult to trace over several days or weeks of transport. As a result statistical relationships between models and ozone sonde measurements are far less satisfactory than for surface measurements at all seasons. The lowest bias between model calculated ozone profiles and the ozone sonde measurements is seen in the winter and autumn months. Following the increase in photochemical activity in the spring and summer months the spread in model results increases and the agreement between ozone sonde measurements and the individual models deteriorates further.

At selected sites calculated contributions to ozone levels in the free troposphere from intercontinental transport are presented. Intercontinental transport is identified based on differences in model calculations with unperturbed emissions and emissions reduced by 20% by region. With emissions perturbed by 20% per region calculated intercontinental contributions to ozone in the free troposphere range from less than 1 ppb to 3 ppb, with small contributions in winter. The results are corroborated by the

ACPD

9, 26095–26142, 2009

retroplume calculations. At several locations the seasonal contributions to ozone in the free troposphere from intercontinental transport differ from what has been shown earlier at the surface using the same dataset. The large spread in model results points to a need of further evaluation of the chemical and physical processes in order to improve the credibility of global model results.

1 Introduction

While local and regional emissions sources are the main cause of air pollution problems worldwide, there is increasing evidence that many air pollutants are transported on a hemispheric or global scale, see (TF HTAP, 2007) and references therein. Observations and model predictions show the potential for intercontinental transport of a number of pollutants such as ozone and its precursors, fine particles, acidifying substances, mercury and POPs (Persistent Organic Pollutants). The Task Force on Hemispheric Transport of Air Pollution (TF HTAP) under the Convention on Long-range Transboundary Air Pollution (LRTAP) has been set up to study these processes. Under the framework of this task force a set of coordinated multi-model studies to address hemispheric transport issues have been defined. These multi model experiments were set up to give a first assessment of the source receptor relationships between the main source regions in the Northern Hemisphere in order to contribute to the revision of the Gothenburg protocol. The model experiments were defined so that all models were run without major adaptations (native resolution, emissions etc.) with year 2001 meteorology. Emissions should be representative of year 2000/2001 conditions. Four regions are defined for source receptor calculations, roughly representing Europe, North America, East Asia and South Asia. Trends in emissions and in pollutant concentrations differ significantly between the selected regions. In the European and North American regions emissions of the pollutants considered are generally decreasing as documented for the individual European and North American countries in WEBDAB (http://www.ceip.at/), whereas in East

ACPD
9, 26095–26142, 2009

Asia and South Asia emissions are in general increasing as documented under ACCESS (http://www.cgrer.uiowa.edu/EMISSION_DATA_new/summary_of_changes.html). As a result the relative distribution of the emissions between the selected regions will now already be markedly different from what they were in 2001, potentially changing the magnitude of trans continental fluxes.

A description of the modelling experiment and key findings are published in the interim report from TF HTAP (TF HTAP, 2007). Furthermore, several papers are already published based on this data set: The contribution from major northern mid-latitude source regions to Arctic pollution (Shindell et al., 2008); hemispheric transport and deposition of oxidised nitrogen (Sanderson et al., 2008); intercontinental source-receptor relationships for surface ozone (Fiore et al., 2009) and the impact of intercontinental ozone pollution on human mortality (Casper-Anenberg et al., 2009). Comparing model surface ozone with observational data, Fiore et al. (2009) found a systematic overestimate of surface ozone levels over the eastern United States and Japan in summer. This bias did not occur in the boreal spring and autumn months when intercontinental transport is strongest, reflecting a combination of more frequent cyclones venting the continents, stronger westerlies and a longer chemical lifetime of ozone compared to the summer months. The spatial average effects of foreign emission reductions in the receptor regions typically range from 0.7–0.9 ppb in spring to 0.3–0.4 ppb in the summer, but effects are likely to be larger on the western part of the continents/regions, closer to the foreign source areas. This was also shown, using the same dataset, in Reidmiller et al. (2009) focusing on North America, where the largest calculated effects of foreign emission reductions were seen in the western parts of the US.

In this paper we evaluate the model vertical profiles of ozone with an extensive measurement programme of vertical soundings for this species. The ozone sondes are primarily launched to study the depletion of the ozone layer in the winter and spring months. As a result measurements are often infrequent or missing in the summer and autumn months at many sites.

Model calculated vertical profiles have been calculated for 32 sites selected based on the availability of ozone soundings. Model calculated ozone profiles are compared to measurements for a subset of four sites located in North America (Goose Bay, and Trinidad Head), Europe (Uccle) and Asia (Yakutsk). The ozone sonde sites presented here (with the exception of Goose Bay) are selected as they are located in the western part of the receptor continent/region in order to get a stronger signal from foreign sources.

Advection of plumes from North America to Europe and from East Asia to North America is conceptually similar and usually involves lifting and subsequent advection in what are denoted as warm conveyor belts (see Stohl and Trickl, 1999; TF HTAP, 2007 and references therein). Across the Atlantic the transport time in the free troposphere is typically three to four days, somewhat longer for transport across the Pacific (TF HTAP, 2007). Transport events of air pollutants from Asia to the western parts of North America typically occur 1–2 times per month (Liang et al., 2004). Such export events can have substantial impacts on concentrations in the free troposphere above the downwind continent. The impact of these transport events on surface sites is however less frequent and dilute (Zhang et al., 2009).

Transport of pollutants from Europe differs from advection across the Atlantic and the Pacific as lifting in frontal systems is less important. Even though advection across the Eurasian continent mainly takes place in the boundary layer, Wild et al. (2004) found the largest contributions to ozone from European sources in the mid troposphere. In the boundary layer ozone is depleted faster as a result of a combination of surface deposition and a shorter chemical lifetime. Yakutsk is located north of 60° N, and may often be located too far north to be fully representative of advection across the Eurasian continent. Advection in general follows isentropic surfaces. Poleward advection (in this case from Europe to semi Arctic Siberia) will tend to ascend in winter and early spring.

Ozone precursors emitted in the four regions considered will affect ozone levels throughout the whole tropospheric column at northern mid latitudes. Once in the free troposphere, the chemical lifetime of ozone is typically one month or more (TF HTAP,

2007; The Royal Society, 2008), much longer than the typical transport times between continents given above. With the long lifetime of ozone it is virtually impossible to trace the ozone pollution in the free troposphere back to any specific source using measurements alone, but rather it will contribute to a hemispheric "cloud of ozone". With the use of models, the origin of ozone in the free troposphere can be estimated as the difference between the reference run and a perturbed run. Different models provide different estimates on the origin of surface ozone in the source receptor calculations as already shown by Fiore et al. (2009).

The advection of the pollutants will in particular be sensitive to the exchange between the boundary layer and the free troposphere above. This in turn will affect the chemical regime in which the pollutants are advected in the models. In the free troposphere the pollutants are detached from the surface and dry deposition is no longer effective. With different timescales in the lifting/mixing process the NO_x to VOC (including CH_4) ratio is likely to change, and thereby the potential for chemical ozone production/destruction. Comparing ozone sonde measurements and model calculations will give further insight to the combined effects of advection and ozone chemistry in the models.

With the use of trajectories, or tracer transport models, the likely origin and advection path of the pollutants can be assessed. This information can enhance our understanding of the measurements and model calculations at the sonde sites, and help explain differences between model results, and also provide information on the predictability of ozone at different sites and height levels.

2 Ozone sonde measurements

With the exception of Yakutsk the ozone sonde data included in this study originates from the World Ozone and Ultraviolet Radiation Data Centre (WOUDC, http://www.woudc.org/). Ozone sonde measurement at Yakutsk have been made within the framework of the THESEO campaign and have been downloaded through the RETRO database (http://nadir.nilu.no/retro/). The most common type of ozonesondes currently

in use are the electrochemical concentration cell (ECC). The ECC ozonesondes are manufactured by EnSci Corp. and Science Pump, with minor differences in construction and some variation in recommended concentrations of the potassium iodide sensing solution and its phosphate buffer. When using the recommended sensing solute concentrations the deviations of tropospheric ozone measurements are expected not to exceed more than a few percent (Smit et al., 2007). At Tateno the KC96 Carbon-Iodine sensors are used. At all other sites ECC instrumentation is used. At both Uccle and Yakutsk EnSci-Z sondes were used with SST0.5 solutions. This is the solution recommended by the producer and also the solution that has been shown to give the best performance for this instrument when compared to a UV-photometer (Smit et al., 2007). As Goose Bay the EnSci-Z sondes were used with 1% KI full buffer solution. This may result in an overestimation of a few percent, but this is largely corrected by the total ozone correction procedure. At Trinidad Head EnSci-2Z were used, also with the solution recommended by the producer. however, the sodium phosphate buffers are diluted to 1/10th of the standard 1% KI sensor solution recipe. At Taipei Science Pump model 6a sondes were used. When properly prepared and handled, ECC ozonesondes have a precision of 3–5% and an absolute accuracy of about 10% in the troposphere (Smit et al., 2007; Deshler et al., 2008). Comparing a range of ozone sondes (Deshler et al., 2008) found that the range in the measurements were generally within 2%, increasing to 4–5% near the surface, tropopause and where ozone gradients were large. The ozone sensor response time (e^{-1}) of about 25 s gives the sonde a vertical resolution of about 100 m for a typical balloon ascent rate of 4 m/s in the troposphere. In the past the accuracy of the ozone sondes was occasionally affected by the interference from SO_2, particularly in Europe. As SO_2 emissions have been reduced this was probably not the case in 2001.

3 The model setup and definition of the model scenario

The twelve models listed in Table 1 have provided model calculated vertical profiles of O_3, CO, NO and NO_2 on the HTAP server.

We use the reference simulation (SRref) and a set of simulations in which emissions of NO_x, CO, and NMVOC were reduced together by 20% within each of four regions (denoted here as SR20%): North America (SR20%NA, 125 W to 60 W and 15 N to 55 N), Europe (SR20%EU, 10 W to 50 E and 25 N to 65 N), East Asia (SR20%EA, 95 E to 160 E and 15 N–50 N) and South Asia (SR20%SA, 50 E to 95 E and 5 N to 35 N). The seven first models (in bold) listed in Table 1 have uploaded vertical profiles also for the SR20% scenarios. The model groups used their own emission estimates in the SRref model simulations.

The analysis of these simulations is supplemented by retroplume calculations with the Lagrangian particle dispersion model FLEXPART version number 8.0 (see Stohl et al., 1998, 2003, 2005, 2007 and http://transport.nilu.no/flexpart for further references) driven by meteorological input data from the European Centre for Medium-Range Weather Forecasts (ECMWF, 2002). These calculations provide quantitative dispersion model runs in time-reversed mode including full turbulence and convection parametrisations. 60 000 particles are released every 250 m in the atmospheric column above the ozone sonde sites from the surface up to 12.5 km altitude. For every height interval, the particles are separately traced backward in time for 20 days, calculating what is denoted as potential emission sensitivity (PES) function in $s\,kg^{-1}$. Since emissions occur predominately at or near the surface, the PES near the surface is particularly important. We therefore show PES values for a so-called footprint layer below 100 m above the surface. By multiplying the PES values with emission fluxes (in $kg\,m^{-2}\,s^{-1}$) for carbon monoxide taken from the EDGAR emission inventory, potential source contribution maps are obtained, which show where surface emissions entered the air mass arriving later at the receptor (not shown). Integration of potential source contributions over continental areas yields simulated carbon monoxide mixing ratios at

ACPD
9, 26095–26142, 2009

the ozone sonde site. These have been examined for the different continental source regions as a function of altitude (not shown), to identify altitude layers with strong influence from foreign emissions.

4 Model results

Previous analysis of the TF HTAP model inter-comparison has mainly focused on the effects on surface concentrations.

Since the models only archived vertical profiles at 32 stations, all of which are located in the northern mid latitudes, we focus here on the impacts of emissions from the NA, EU, and EA regions. As seen in Sect. 4.1, the contribution from emissions in SA to tropospheric ozone is small at northern mid latitudes.

Figure 1 shows the mean change in annual mean ozone, calculated with the seven first models listed in Table 1, in the lower free troposphere (750 hPa) when NO_x, CO, and NMVOC are decreased by 20% in the NA, EU and EA regions. Once in the free troposphere emissions from the three areas are advected much further than in the boundary layer due to a longer lifetime of ozone, combined with higher wind speeds. Emissions from NA, EU and EA are mostly advected in the westerlies and consequently regions east of the source areas are the most affected. However, effects can be seen throughout the northern mid and high latitudes at this level.

Below we evaluate the ozone simulations with the ozone soundings. Furthermore we highlight long range transport events, as diagnosed from differences between the ozone vertical profiles in the SRref and SR20% scenarios, for selected dates at Goose Bay, Uccle, Trinidad Head and Yakutsk. This analysis is extended to also include retroplume calculations with the FLEXPART model.

4.1 Model evaluation by ozonesondes

In Table 2 ozone sondes and vertical profiles calculated with the models listed in Table 1 are compared for Goose Bay, Uccle, Trinidad Head and Yakutsk. Only days with measurements are included in the comparison (This dataset is also included as Figures in the supplementary material: http://www.atmos-chem-phys-discuss.net/9/26095/2009/acpd-9-26095-2009-supplement.pdf, including also data for the Summer and Autumn). In Figs. 2 to 5 the daily range of ozone calculated by the same models is shown. At the right hand side of these figures specific events/episodes are highlighted. These events/episodes are described in more detail in later sections. In the figures the sonde measurements are marked as black dots showing that at most sites the frequency of sonde measurements is highest in winter and spring. There are large differences in the frequencies of sondes released at the sites. At Uccle there are sonde measurement made almost every second day throughout the year, whereas for the other sites sonde measurements are infrequent or missing in particular in the summer months. Therefore we only include data for the first two seasons in Table 2 (The same dataset for all seasons, and the year as a whole, are visualised in the supplementary material: http://www.atmos-chem-phys-discuss.net/9/26095/2009/acpd-9-26095-2009-supplement.pdf). Even so the comparisons with measurements in Table 2 are based on very few data for some of the sites.

The data presented in Table 2, and the supplementary material: http://www.atmos-chem-phys-discuss.net/9/26095/2009/acpd-9-26095-2009-supplement.pdf are supplemented by Taylor diagrams (Figs. 6 and 7). Detail about the use of Taylor diagrams are provided in (Taylor, 2001) and on the NCL homepage: (http://www.ncl.ucar.edu/Applications/taylor.shtml). The Taylor diagrams are not divided into season, but as there are more measurements in winter and early spring there is a clear bias to the winter months in the Taylor diagrams. In addition to correlation with measurements the Taylor diagrams show the RMS error and the normalised standard deviations. There is considerable scatter in the results presented in the Taylor diagrams.

As ozone sonde errors are expected to be of the order of a few percent only (Sect. 2) the scatter can be ascribed to model errors. One general feature for virtually all models and sites is that the standard deviation is low in the upper troposphere compared to the ozone sondes. This may be related to coarse model resolution (both vertical and horizontal) resulting in too little variability in the UTLS region. With a low chemical activity the range in calculated ozone as seen in the Figs. 2 to 5 are small in the autumn and winter months. As the chemistry becomes active in the spring and summer months, the spread in model results increases, and clear over and underestimations compared to ozone soundings and/or model median results become more apparent in the daily calculated ozone. The seasonal averages in winter and spring for most models are well within a 20% compared to the sonde measurements in the lower and middle troposphere. In the upper troposphere the bias is often higher (see Table 2 and supplementary material: http://www.atmos-chem-phys-discuss.net/9/26095/2009/acpd-9-26095-2009-supplement.pdf). The spread in model results are caused by a combination of differences in chemical formulation and by differences in the advection emphasised as the range between low and high ozone regions increase.

Based on the comparison with measurements in Table 2 (and the supplementary material: http://www.atmos-chem-phys-discuss.net/9/26095/2009/acpd-9-26095-2009-supplement.pdf and the Taylor diagrams in Figs. 6 and 7, the best model performance is seen for Goose Bay. This site is on the eastern side of the North American continent with major North American source regions close enough for the plumes reaching this site to maintain their identity in the models, but still sufficiently far away for lifting and mixing into the free troposphere to take place, resulting in relatively low RMS errors and high correlations with the measurements compared to the other sites. The models also perform reasonably well for Uccle. These soundings are made directly above one of the highest emitting regions in Europe, and in particular in the lower troposphere results are affected by these local and regional sources. For Trinidad Head it is unfortunate that there are no sondes released after 18 May. Even though domestic (North American) sources contribute the most for

extended periods in summer and autumn in the lower and partially in the middle troposphere, the trans continental contributions are large (see discussion in Sect. 4.6) and model performance is not as good as Goose Bay and Uccle at this site. The least satisfactory performance is found for the remote site Yakutsk where there are virtually no correlations between models and ozone sonde measurements in winter and spring at all height levels. In addition Taylor diagrams are included for Tateno (36.05° N, 140.10° E) in Japan, and Taipei (25.032° N, 121.53° E) on Taiwan in Fig. 7. Model performance at these two sites are similar to that of Uccle and Goose Bay. Ozone at these two sites are affected by a combination of large local sources and sources at the East Asian mainland. As shown by the range in calculated ozone in the Figs. 2 to 5, there are significant differences in the ability of the models to reproduce ozone levels at the different sites. Even though the seasonal differences between models and sonde measurements are moderate, the day by day difference is considerably larger. Most of the sonde measurements fall within the displayed model range. In the lower and middle troposphere the range is more narrow in the autumn and winter months. Measurements outside this range reflect specific events not included in the models. Nearly all of the incidents where measured ozone is notably outside the range, are in the upper troposphere, and are probably associated with misplaced tropopause heights or stratospheric intrusion events. The low value measured in late May at Uccle (Fig. 3) was probably caused by ozone titration, as regional NO_x emissions are very high in this part of Europe. In Fiore et al. (2009) and in Reidmiller et al. (2009) it was shown that the models have considerable skills in reproducing measured ozone for surface sites. In the boundary layer the lifetime of ozone is of the order of days only, and ozone is strongly affected by regional sources. The subset from the same set of models, included in this study, have far more difficulty in accurately reproducing ozone variability in the free troposphere. Similar results were also demonstrated in Tarasick et al. (2007) for two Canadian operational air quality models (not represented in this study) and by Tong and Mauzerall (2006) for the community AQ model CMAQ. In Stevenson et al. (2006) it was shown that a model ensemble was

able to reproduce the monthly mean ozone levels in the free troposphere. As shown in Table 2, the supplementary material: http://www.atmos-chem-phys-discuss.net/9/26095/2009/acpd-9-26095-2009-supplement.pdf and in Figs. 2 to 5 most models (and subsequently the model mean) included here reproduce the mean abundances and seasonal cycle of ozone in a similar fashion to what was shown in Stevenson et al. (2006). Liu et al. (2009) calculated the correlations between nearby pairs of sonde stations. They found low correlations near the surface indicating that local and regional effects are important here. From the surface correlations rose sharply to a local maximum in the lower troposphere. This implies that the measurements here will be representative for a larger area, reducing the disadvantage of using relatively coarse models, but assuming that errors will propagate in space (and time) the extensive spatial range of influence for long lived pollutants may be too large for the models to reproduce. There are marked differences between the individual sites in the model statistics as RMS errors and correlations with measurements. We believe these differences largely reflects the proximity of the dominant sources affecting the sites. With the largest contributions from trans continental sources, located much further away, the identity of the ozone plumes are partially lost as they are advected over large distances. This loss of identity are likely to be caused by a combination of factors such as inaccuracies in the meteorological driver, inaccuracies stemming from the interpolation in time of the meteorological fields and the parameterisation of the advection processes in the CTMs. The lack of stratification in the model calculated profiles compared to the ozone sondes as seen in the Figs. 8a, 9a, 10a and 11a may serve as an illustration of such effects. Furthermore uncertainties in emissions and chemistry will add to the lack of agreement between models and measurements. Such errors will propagate in time. This could in part explain the high RMS errors and low correlations at some sites as discussed above. There is in general less agreement between models and measurements in the upper troposphere. In particular in the upper troposphere intrusion of stratospheric air will bring air with high ozone content to the sites. This is not always well represented in dynamical models, particularly those

with moderate resolutions. Moreover, as already noted, the lifetime of ozone is much longer in the upper troposphere. Model discrepancies in the upper troposphere will mostly be due to poor resolution of the timing, location and magnitude of stratospheric intrusions. At lower latitudes ozone levels are usually low throughout the tropospheric column. Thus airmasses of tropical or subtropical origin will in general have a low ozone content that may not be captured by the models. As noted in Sect. 2 ozone levels in the boundary layer and lower troposphere could be subject to local effects not resolved in global models, and this could partially explain the somewhat lower model to sonde correlation in the lower troposphere. In the lower troposphere there is some tendency for the models with the highest resolution to capture some of this effect, performing better for those sites affected by regional sources. In the upper troposphere there is a tendency for many models to overpredict ozone levels in the winter and underpredict in spring. The spin-up for most of the models were made with meteorological data for the year 2001, and not with 2000 meteorological data. For most models this implies that the concentrations in the first part of January will not reflect the meteorological evolution from previous days or weeks, to some extent affecting correlations with measurements in the first part of the winter months.

4.2 Goose Bay: tracing plumes within the North American continent

This site is located at 53.32° N and 60.13° W. Even though this site is within the NA region as defined in Sect. 3 it is well outside major US and Canadian source regions, but as also shown in Sect. 4.6, these sources contribute significantly to ozone levels above this site. As such this site is well suited for identifying transport events within the North American continent. As an example of advection to this site 13 June 2001 has been selected. In Fig. 8a the model calculated vertical profiles are compared to the ozone sounding. The ozone soundings and most of the models show high ozone levels in the lower troposphere for this date. Furthermore, in Fig. 8b the models show reductions of the order of 2–5.5 ppb in the lower troposphere from 20% reductions in NA emissions (SR20%NA scenario, as defined in Sect. 3). The model range in calculated ozone

and the ozone sondes are shown in the right hand part of Fig. 2 for the lower, middle and upper troposphere for a two week period centered around 13 June. For the same height intervals the model range in the contributions from domestic and transcontinental regions is also shown. At this site the dominant calculated contributions to ozone at all levels are from the domestic NA region throughout this period.

The footprint emission sensitivity for Goose Bay for the lower part of the troposphere (release height 0–250 m) at 12:00 UTC on 13 June (Fig. 8c) indicates that the sources of ozone/ozone precursors near the surface, also seen as excess ozone in the lower troposphere in Fig. 8b, can be traced to emissions at the US east coast and around the Great Lakes a few days earlier. Figures 8d and e shows the difference in calculated daily maximum ozone at the surface and the difference in total ozone column in the troposphere respectively, between SRref and SR20%NA calculated with the EMEP model. It shows enhanced daily maximum ozone levels at and around Goose Bay. Whereas there are only small changes in the total tropospheric column directly above Goose Bay.

4.3 Uccle: tracing trans Atlantic advection

Uccle is located at 50.48° N and 4.21° E in Belgium, in the western part of Europe. As discussed in Sect. 4.6 the largest calculated contribution in the middle and upper troposphere is from the NA region. As an example of advection to this site we have selected 1 June as there are ozone soundings for this date (Fig. 9a). Except for one model the ozone sonde measurements are rather well reproduced by the numerical simulations, but the elevated ozone in the upper troposphere is not fully accounted for by the models. All models do however show a 1 ppb or more contribution from a 20% reduction in North American emissions (Fig. 9b) in the mid and upper troposphere suggesting that this excess ozone could be of North American origin. The model range in calculated ozone and the ozone sondes are shown in the right hand part of Fig. 3 for the lower, middle and upper troposphere for a two week period centred around 1 June. For the same height intervals the model range in the contributions from domestic and

transcontinental regions is also shown. At this site the main contributions to ozone at all height intervals are transcontinental (mainly from the NA region) throughout this period, with the largest contributions around 1 June.

Figure 9c shows the footprint emission sensitivity for retroplumes released in the middle troposphere, between 5250 and 5500 m. At this level the retroplumes indicate that there are marked contributions from the North American continent as also seen in Fig. 9b.

Figure 9d and 9e show the difference between the reference run SRref and SR20%NA in daily maximum surface ozone and total tropospheric ozone column calculated by the EMEP Unified model for noon, 1 June. At the surface there is virtually no contribution from North America to the daily maximum ozone, as also shown in Fig. 9b for all the models. For the tropospheric ozone column there is a marked difference attributed to contributions from North America extending to western Europe.

4.4 Trinidad Head: tracing trans Pacific advection of ozone

Trinidad Head is located at 41.05° N and 124.15° W, at the west coast of North America. In Sect. 4.6 it is shown that the largest calculated contribution to ozone in the middle and upper troposphere originates from the EA region at this site, making this location well suited for detecting trans Pacific pollution events. Transport events of air pollutants from Asia to the western parts of North America typically occur 1–2 times per month, predominantly in the middle and upper free troposphere (Liang et al., 2004). As an example of such events 23 April has been selected. Unfortunately no ozone sounding was available for this particular date. As is typical for spring and summer conditions, the spread in model calculated ozone profiles is relatively large (Fig. 10a). The model calculated difference in the vertical ozone profiles between the reference model run and the model runs with reduced emissions in East Asia (SR20%EA) is somewhat less than 1 ppb throughout the troposphere for all models except one (Fig. 10b). The model range in calculated ozone and the ozone sondes are shown in the right hand part of Fig. 4 for the lower, middle and upper troposphere for a two week period cen-

tred around 23 April. For the same height intervals the model range in domestic and transcontinental contributions to ozone is also shown. At this site the main calculated contributions to ozone at all height intervals are transcontinental (mainly from the EA region) throughout this period.

The footprint emission sensitivity for Trinidad Head at 12:00 UTC on 13 June (Fig. 10c) with retroplumes released in the lowest 250 m indicates that approximately 1 ppb excess ozone calculated throughout much of the troposphere in Fig. 10b can be attributed to emissions in East Asia. The main source regions in this area are located at or near the Pacific rim. The difference in daily maximum surface ozone calculated with the EMEP model between SRref and the model run reducing all emission in East Asia by 20% are shown in Fig. 10d. The effects on daily maximum ozone is of the order of 0.5 ppb throughout much of the Pacific, with a tongue of excess ozone of 2–3 ppb just west of the North American continent. This tongue is seen throughout the tropospheric column (Fig. 10e) covering also parts of the North American continent.

4.5 Yakutsk: tracing trans Eurasian emissions

Yakutsk is located at 62.008° N 129.75° E, in the Siberian part of Russia. This site was selected for tracing plumes from Europe across the Eurasian continent. As discussed in the introduction, ozone from the EU region is primarily advected in the lower atmosphere where the lifetime is markedly shorter than in the free troposphere. It is therefore difficult to identify specific transport events from EU to this site. As an example of ozone reaching this site 9 May was chosen, as all the models calculated a significant contribution from the EU region based on the difference in vertical ozone profiles. In the free troposphere all models calculate an ≈1 ppb difference between SRref and SR20%EU, reducing all emissions in the European region (Fig. 11b). Unfortunately no ozone sounding is available for this date at Yakutsk. Vertical profiles calculated by the models are shown in Fig. 11a. The model range in calculated ozone and the ozone sondes are shown in the right hand part of Fig. 5 for the lower, middle and upper troposphere for a two week period centred around 9 May. For the same height intervals

the model range in the transcontinental contributions to ozone is also shown. As this site is outside all of the regions specified in Sect. 3 there are no calculated domestic contributions, and all the calculated contributions are transcontinental. Throughout the two weeks period the largest calculated contributions to ozone are from the EA region, in particular in the lower troposphere, but there are also variable contributions from the EU region.

Footprint emission sensitivity retroplumes with release height below 250 m are shown in Fig. 11c). A substantial fraction of the air can be traced back to the Scandinavian countries. The potential for forming ozone from this region is small due to low emissions of ozone precursors and low insolation. There is also a relatively high emission sensitivity over central parts of Europe, where emissions of ozone precursors are higher. The difference in daily maximum ozone between SRref and SR20%EU calculated with the EMEP model for 9 May (Fig. 11d) is typically about 0.5 ppb in large parts of Asia, with signs of plumes of more than 1 ppb advected in the boundary layer further west and south. For the tropospheric ozone column the difference plot between SRref and SR20%EU (Fig. 11e) show plumes advected in the vicinity of Yakutsk.

4.6 Intercontinental transport

In Figs. 12 to 15 the seasonal contributions to ozone from 20% reductions in the emissions in the four source regions are shown for the same sonde sites as in Table 2 based on the daily vertical profiles from seven numerical models at noon. Winter includes January and February. Spring: March, April and May, Summer: June, July, August and Autumn: September, October, November. In addition the daily model mean contributions are shown in Figs. 2 to 5. As in Table 2, the data are separated into lower, middle and upper troposphere. The calculated trans-continental contributions from 20% reductions in emissions shown in Figs. 12 to 15 are often in the 0.5–1 ppb range, with contributions for some sites and models well above 1 ppb. The seasonality of the trans

continental (or foreign) contributions in the free troposphere differ between the sites, but for all sites and models the contributions are small in winter.

The trans continental contributions are episodic in their nature, and care should be taken as the data are based on one year only.

Two of the sonde sites, Goose Bay and Trinidad Head are located in the NA region. The magnitude of the model mean foreign impact (from EA, SA and EU) differ between the two sites. At Trinidad Head the model mean foreign impact is highest in spring, adding up to about 1 ppb or more at all levels. In the upper and mid troposphere the foreign impact is only slightly reduced in summer. Above Goose Bay the foreign impact is always lower and about 0.8 ppb in spring. Contrary to Trinidad Head the foreign impact is markedly lower in summer. The higher foreign impact at Trinidad Head is mainly caused by larger contributions from the EA region. As can be expected the foreign impact in the free troposphere is higher than what was calculated for NA at the surface in Fiore et al. (2009). Within the United states Reidmiller et al. (2009) found the largest foreign impact in the Western United States in spring with about 0.9 ppb. In summer the foreign impact fell to about 0.5 here. In the Eastern United States the calculated foreign impact was about half that of the Western United states. The results presented here are in good agreement with Holzer et al. (2005) where they found that the surface signal of East Asian sources is strongest in spring, and that East Asian air is transported aloft in summer. In a general eastward circulation air having been exposed to loss processes in the boundary layer is mixed into the free troposphere through increased venting over the continent in the summer, reducing the foreign contribution to ozone also in the free troposphere. As a result sites at the eastern side of the continent have a summer minimum in foreign ozone throughout the tropospheric column, whereas sites located at the western side of the US continent (as Trinidad Head) will have a marked summer minimum in the foreign impact only near the surface.

At Uccle, in the western part of Europe, the calculated trans continental contributions in the middle and upper troposphere are larger than the domestic contributions (up to

about 1 ppb or more at all levels with NA as the largest single source). In the lower troposphere the largest contributions are from domestic sources in most of the year. The larger contribution in the free troposphere compared to what was calculated as foreign impact to EU at the surface in Fiore et al. (2009) can partially be explained by Uccle being located close to the windward margin of the EU domain, and partially because of higher trans continental contributions in the free troposphere. A higher foreign contribution in the free troposphere is in good agreement with Auvray and Bey (2005). They found a maximum in ozone from North America in Spring and summer. As a result of deep convection in summer they found a high contribution from North American ozone at high altitudes. The low level advection of ozone across the North Atlantic was found to be important only in spring, when loss rates in the boundary layer are weaker.

In winter the advection to Yakutsk is dominated by the Siberian high, with airmasses crossing the Eurasian continent, potentially advecting pollution of European origin to Yakutsk. But in the winter months the chemical activity is very low resulting in low contributions to ozone levels above Yakutsk from all the four source regions. From Europe a major part of the pollutants are advected in the boundary layer or lower troposphere where the lifetime of ozone is short. Following the breakdown of the Siberian high in Spring, the foreign impacts calculated above Yakutsk, of the order of 2 ppb, are the highest among all the sites. The largest contributions at Yakutsk are now from EA at all levels. As Goose Bay, Uccle and Trinidad Head are located within the NA or EU domains, domestic contributions are not included, even though airmasses of domestic origin may in fact have encircled the globe thus being of intercontinental nature. At Yakutsk all four source regions are foreign, and this could partially explain the higher impact here. The attribution of sources to Yakutsk differs from that of Mondy described in Wild et al. (2004) as it seems to receive less pollution from Europe. Yakutsk is located about 20° further east, and receives a much large portion of its pollution from EA, and as a result this site is less ideal for identifying pollutant transport from Europe. Paris et al. (2008) also found that advection of boundary layer air exposed to Asian

emissions and lifted by Warm Conveyor Belt contributed significantly to CO and CO_2 enhancements in the upper troposphere in Siberia during the YAK-AEROSIB aircraft campaigns in April 2006.

The contributions from trans continental pollution for individual episodes shown in Figs. 8b–11b gives an impression of a better agreement between the models than the Figs. 12 to 15. The episodes presented in Figs. 8b–11b are however chosen because of particular strong signals in the contributions from selected regions and illustrates that the models have predictability on a hemispheric scale for such events. The episodes chosen showing trans continental contributions to Uccle (Sect. 4.3), Trinidad Head (Sect. 4.4) and Yakutsk (Sect. 4.5) illustrates typical mechanisms for these events. Trans Atlantic advection to Uccle and trans Pacific advection to Trinidad Head are resulting from lifting near the east coast of the source continent and subsequent advection in the free troposphere to the receptor sites. The selected episode with Advection to Yakutsk is characterised by more shallow advection and a much smaller signal.

5 Conclusions

When averaging over an ensemble, numerical simulations are capable to reproduce the ozone climatology in the free troposphere in the Northern Hemisphere. At the same time the models have limited abilities in reproducing the day by day variability in ozone. For the models to reproduce the daily variability of ozone at the same level of detail as for surface sites require accurate calculations describing the development of ozone plumes over days to weeks or longer, at the limit of the capabilities of present CTM's and also at the limit of the capabilities of the underlying numerical weather prediction models. The study shows, that the capabilities of the individuals models to describe day to day ozone variability strongly depends on the individual model, yielding for some models poor correlations which needs further study.

Comparing model calculated vertical profiles with ozone sonde measurements, there are clear indications that this ability is partially determined by the distance to the

dominant source region(s) affecting ozone at the individual site and level. As an example the highest correlations are calculated for Goose Bay. As shown in Sect. 4.6 the major model calculated source regions to this site are within the NA region, close enough to maintain the identity of the plumes, and thus the relatively short distance makes it easier for the models to determine source receptor relationships.

As demonstrated in Sects. 4.3 and 4.4 for the selected days the effects of North American emissions on ozone above Uccle and East Asian emissions above Trinidad Head were predominantly restricted to the free troposphere. For Trinidad Head the trans continental contributions calculated here for the three height levels are markedly higher than the contribution to The Northwest and California regions at the surface based on the same dataset in Reidmiller et al. (2009). A less frequent and dilute impact at the surface compared to the free troposphere was also seen by Zhang et al. (2009), comparing advection to Mt. Bachelor at 2.7 km altitude, and to Trinidad Head at sea level.

As discussed in Sect. 4.6 the trans continental contribution of ozone in the free troposphere is larger, and with a different seasonality, compared to what was calculated for the surface in Fiore et al. (2009) and Reidmiller et al. (2009). In summer the loss rates in the boundary layer are high and ozone will not be advected between continents at this level. As a result of convection in the eastern parts of the continents air rich in ozone and ozone precursors is lifted to high altitudes in summer and advected across the Atlantic/Pacific oceans. A major portion of the exchange of ozone between the continents take place at high altitude and here advection is not significantly weakened in summer, but as (excess) ozone is mixed down into the boundary layer it is partially lost through surface deposition and chemistry. Mixing of ozone between the boundary layer and free tropospheric air as air masses are advected across the North American continent could be the reason for difference in seasonality between Trinidad Head and Goose Bay as discussed in Sect. 4.6.

The attribution of the effects on ozone to to the source regions by the TF HTAP models is corroborated by the FLEXPART retroplume calculations. For the appropriate height levels where the effects of emission reductions in one of the four regions are seen in the HTAP model calculations, the retroplume calculations also indicates a marked contribution from the same area. But as the plumes are advected over long distances they eventually lose their identity as individual plumes and can no longer be traced back to their exact origin as demonstrated by the FLEXPART retroplume calculations. The retroplume eventually splits into multiple pathways and the tracer can no longer be ascribed to any given source region with any degree of certainty. Calculated difference in vertical ozone profiles shows that even so there is virtually always a difference between the reference SRref and the SR20% scenarios. This excess ozone may be viewed as contributing to the persistant background ozone encircling the northern mid latitudes as a whole. The hypothesis above will need further study.

The calculated effects of 20% reductions in the emissions in the four selected regions result in trans continental reductions in free tropospheric ozone often in the 0.5–1 ppb range, with seasonal contributions for some models and sites well above 1 ppb. Scaling the 20% emission perturbations to 100% (as in Figs. 2 to 5) suggests that the total contributions from trans-continental transport are of the order of 2.5–5 ppb. However, the ozone chemistry is strongly non-linear, so these contributions may in fact be larger. Derwent et al. (2004) compared a tracer labelling technique with the effects of 50% reductions in emissions in North America and Asia. They found that the tracer labelling technique gave higher estimates, and argues that this gives a more realistic quantification of intercontinental transport. On the other hand, using percentage reductions in the source regions gives a more policy relevant quantification by describing potential responses to emission control.

For Goose Bay and Uccle correlations with measurements in the lower troposphere tends to be linked to the model resolution. At the same two sites the magnitude of ozone that can be attributed to North American sources is also weakly linked to model resolution. The magnitude of the trans-continental contributions from other regions

or for other sites can not be linked to model resolution. There appears to be no relationship between model to measurement statistics (such as bias, correlations and variance) and the magnitude of trans-continental pollution.

Even though all models agree that there are marked trans continental contributions, there are large differences between the individual models. Large differences between the models was also found in the assessment of pollution transport to the Arctic (Shindell et al., 2008). Further analysis is required to unveil the reasons for these differences. When comparing the effects of emission reductions in the regions in Figs. 12 to 15 to the bias in Table 2 and the supplementary material: http://www.atmos-chem-phys-discuss.net/9/26095/2009/acpd-9-26095-2009-supplement.pdf, there is no apparent connection between model bias and the magnitude in the response to the SR20% reductions in the emissions of ozone precursors, confirming the results of Fiore et al. (2009) when comparing model results with surface ozone measurements over the eastern United States and model response to emission changes.

The use of ensemble models often result in better agreements with measurements, and as such may give more reliable predictions. But more reliable predictions can only be achieved by further improvements in the individual models included in the ensemble mean. This can only be achieved by carefully evaluating model performance for all available species and measurement platforms. In particular it is very difficult to evaluate the reliability of the model results concerning intercontinental ozone transport, as the calculated perturbations in ozone are in the range of percents (or less), and the spread in model predictions are of the same order.

Clearly more work is needed improving the predictive potentials of the models through evaluation comparing with measurements of all available species measurement platforms. Differences in magnitude between the models are results of complicated interactions between advection, including vertical exchange processes, and chemistry involving species with a wide range of chemical lifetimes. It may however prove difficult to identify direct observational-based constraints alone to select the mod-

els that best represent hemispheric ozone transport. In addition the parameterisation of these processes should be compared separately in the models. A total of 19 global models (several of them included in this study) have uploaded model results for a chemical tracer experiments with tracer lifetimes ranging from 50 days (CO like) to a few days (VOC like). This tracer experiment may help explain some of the differences between the models. One option to further untangle these differences could be a proposed transition to reality model experiment, extending the tracer experiment by adding more chemistry, successively bringing these runs into closer alignment with real tropospheric chemistry calculations as simulated during the standard SRref simulation of HTAP. The differences between the models will then escalate as more detail is included in the calculations, and help determining the main processes causing the large spread in model results.

Several companion papers are already published based on the data sets in the HTAP database, and several additional papers are in progress. Furthermore a final report from the TF HTAP task force will be published in 2010 synthesising the findings from these publications.

Acknowledgements. This work was supported by the Co-operative Programme for Monitoring and Evaluation of the Long-range Transmission of Air pollutants in Europe (EMEP) under UNECE. We would like to thank Åsmund Fahre Vik, NILU and Johannes Stähelin, ETH Zürich, for valuable advice on the interpretation of ozone sonde data. We would also like to thank WOUDC for making the ozone sonde measurements available. The ozone sounding program in Uccle is supported by the Solar-Terrestrial Centre of Excellence, a research collaboration established by the Belgian Federal Government through the action plan for reinforcement of the federal scientific institutes (decision council of ministers taken on 22 March 2006).

References

Auvray, M. and Bey, I.: Long-range transport to Europe: Seasonal variations and implications for the European ozone budget, J. Geophys. Res., 110, D11303, doi:doi:10.1029/2004JD005503, 2005. 26115

Casper-Anenberg, S., West, J., Fiore, A., Jaffe, D., Prather, M., Bergman, D., Cuvalier, K., Dentener, F., Duncan, B., Gauss, M., Hess, P., Jonson, J., Lupu, A., MacKenzie, I., Marmer, E., Park, R., Sanderson, M., Schultz, M., Shindell, D., Szopa, S., Vivanco, M., Wild, O., and Zeng, G.: Intercontinental impacts of ozone pollution on human mortality, Environ. Sci. Technol., 43(17), doi:10.1021/es900518z, 2009. 26099

Derwent, R., Stevenson, D., Collins, W., and Johnson, C.: Intercontinental transport and the origins of the ozone observed at surface sites in Europe, Atmos. Environ., 38, 1891–1901, 2004. 26118

Deshler, T., Mercer, J., Smit, H., Stubi, R., Levrat, G., Johnson, B., Oltmans, S., Kivi, R., Thompson, A., Witte, J., Davies, J., Schmidlin, F., Brothers, G., and Sasaki, T.: Atmospheric comparison of electrochemical cell ozonesondes from different manufacturers, and with different cathode solution strengths: The Ballon Experiment on Standards for Ozonesondes, J. Geophys. Res., 113, D04307, doi:10.1029/2007JD008975, 2008. 26102

ECMWF: edited by: White, P. W.: IFS Documentation, ECMWF, Reading, UK, 2002. 26103

Fiore, A., Dentener, F., Wild, O., Cuvelier, C., Schultz, M., Textor, C., Schulz, M., Atherton, C., Bergmann, D., Bey, I., Carmichael, G., Doherty, R., Duncan, B., Faluvegi, G., Folberth, G., Garcia Vivanco, M., Gauss, M., Gong, S., Hauglustaine, D., Hess, P., Holloway, T., Horowitz, L., Isaksen, I., Jacob, D., Jonson, J., Kaminski, J., Keating, T., Lupu, A., MacKenzie, I., Marmer, E., Montanaro, V., Park, R., Pringle, K., Pyle, J., Sanderson, M., Schroeder, S., Shindell, D., Stevenson, D., Szopa, S., Van Dingenen, R., Wind, P., Wojcik, G., Wu, S., Zeng, G., and Zuber, A.: Multi-model estimates of intercontinental source-receptor relationships for ozone pollution, J. Geophys. Res., 114, D04301, doi:10.1029/2008JD010816, 2009. 26099, 26101, 26107, 26114, 26115, 26117, 26119

Holzer, M., Hall, T., and Stull, R.: Seasonality and weather-driven variability of transpacific transport, J. Geophys. Res., 110, D23103, doi:10.1029/2005JD006261, 2005. 26114

Liang, Q., Jaegle, L., Jaffe, D., Weiss-Penzias, P., and Heckman, A.: Long-range transport of Asian pollution to the northeast Pacific: Seasonal variations and transport pathways of carbon monoxide, J. Geophys. Res., 109, D23S07, doi:10.1029/2003JD004402, 2004. 26100,

26111
Liu, G., Tarasick, D., Fioletov, V., Sioris, C., and Rochon, Y.: Ozone correlations lengths and measurement uncertainties from analysis of historical ozonesonde data in North America and Europe, J. Geophys. Res., 114, D04112, doi:10.1029/2008JD010576, 2009. 26108
Paris, J., Ciais, P., Nedéléc, P., Ramonet, M., Belan, B., Arshinov, M., Golitsyn, G., Granberg, I., Stohl, A., and Cayez, G.: The YAK-AEROSIB transcontinental aircraft campaigns: new insights on the transport of CO_2, CO and O_3 accross Siberiak, Tellus B, 60, 551–568, 2008. 26115
Reidmiller, D. R., Fiore, A. M., Jaffe, D. A., Bergmann, D., Cuvelier, C., Dentener, F. J., Duncan, B. N., Folberth, G., Gauss, M., Gong, S., Hess, P., Jonson, J. E., Keating, T., Lupu, A., Marmer, E., Park, R., Schultz, M. G., Shindell, D. T., Szopa, S., Vivanco, M. G., Wild, O., and Zuber, A.: The influence of foreign vs. North American emissions on surface ozone in the US, Atmos. Chem. Phys., 9, 5027–5042, 2009, http://www.atmos-chem-phys.net/9/5027/2009/. 26099, 26107, 26114, 26117
Sanderson, M., Dentener, F., Fiore, A., Cuvelier, K., Keating, T., Zuber, A., Atherton, C., Bergmann, D., Diehl, T., Doherty, R., Duncan, B., Hess, P., Horowitz, L., Jacob, D., Jonson, J., Kaminski, J., Lupu, A., Mackenzie, I., Mancini, E., Marmer, E., Park, R., Pitari, G., Prather, M., Pringle, K., Schroeder, S., Schultz, M., Shindell, D., Szopa, S., Wild, O., and Wind, P.: A multi-model study of the hemispheric transport and deposition of oxidised nitrogen, Geophys. Res. Lett., 35, L17815, doi:10.1029/2008GL035389, 2008. 26099
Shindell, D. T., Chin, M., Dentener, F., Doherty, R. M., Faluvegi, G., Fiore, A. M., Hess, P., Koch, D. M., MacKenzie, I. A., Sanderson, M. G., Schultz, M. G., Schulz, M., Stevenson, D. S., Teich, H., Textor, C., Wild, O., Bergmann, D. J., Bey, I., Bian, H., Cuvelier, C., Duncan, B. N., Folberth, G., Horowitz, L. W., Jonson, J., Kaminski, J. W., Marmer, E., Park, R., Pringle, K. J., Schroeder, S., Szopa, S., Takemura, T., Zeng, G., Keating, T. J., and Zuber, A.: A multi-model assessment of pollution transport to the Arctic, Atmos. Chem. Phys., 8, 5353–5372, 2008, http://www.atmos-chem-phys.net/8/5353/2008/. 26099, 26119
Smit, H., Straeter, W., Johnson, B., Oltmans, S., Davies, J., Tarasick, D. W., Hoegger, B., Stubi, R., Schmidlin, F., Northam, T., Thompson, A., Witte, J., Boyd, I., and Posny, F.: Assessment of the performance of ECC-ozonesondes under quasi-flight conditions in the environmental simulation chamber: Insights from the Juelich Ozone Sonde Intercomparison Experiment (JOSIE), J. Geophys. Res., 112, D19306, doi:10.1029/2006JD007308, 2007. 26102

Stevenson, D., Dentener, F., Schultz, M., Ellingsen, K., van Noije, T., Wild, O., Zeng, O., Amann, M., Atherton, C., Bell, N., Bergmann, D., Bey, I., Butler, T., Cofala, J., Collins, W., Doherty, R. D. R., Drevet, J., Askes, H., Fiore, A., Hauglustaine, M. G. D., Horowitz, L., Isaksen, I., Lamarque, M. K. J., Lawrence, M., Monanaro, V., Müller, J., Pyle, G. P. M. P. J., Rast, S., Rodriguez, J. M., Sanderson, M., Savage, N., Shindell, D., Strahan, S., Sudo, K., and Szopa, S.: Multimodel ensemble simulations of present-day and near-future tropospheric ozone, J. Geophys. Res., 111, D08301, doi:10.1029/2005JD006338, 2006. 26107, 26108

Stohl, A. and Trickl, T.: A textbook example of long-range transport: Simultaneous observation of ozone maxima of stratospheric and North American origin in the free troposphere over Europe, J. Geophys. Res., 104, 30445–30462, 1999. 26100

Stohl, A., Hittenberger, M., and Wotawa, G.: Validation of the Lagrangian particle dispersion model FLEXPART against large scale tracer experiment data, Atmos. Environ., 32, 4245–4264, 1998. 26103

Stohl, A., Forster, C., Eckhart, S., Spichtinger, N., Huntrieser, H., Heland, J., Schlager, H., Wilhelm, S., Arnold, F., and Cooper, O.: A backward modeling study of intercontinental pollution transport using aircraft measurements, J. Geophys. Res., 108, D12, doi:10.1029/2002JD002862, 2003. 26103

Stohl, A., Forster, C., Frank, A., Seibert, P., and Wotawa, G.: Technical note: The Lagrangian particle dispersion model FLEXPART version 6.2, Atmos. Chem. Phys., 5, 2461–2474, 2005, http://www.atmos-chem-phys.net/5/2461/2005/. 26103

Stohl, A., Berg, T., Burkhart, J. F., Fjæraa, A. M., Forster, C., Herber, A., Hov, Ø., Lunder, C., McMillan, W. W., Oltmans, S., Shiobara, M., Simpson, D., Solberg, S., Stebel, K., Ström, J., Tørseth, K., Treffeisen, R., Virkkunen, K., and Yttri, K. E.: Arctic smoke - record high air pollution levels in the European Arctic due to agricultural fires in Eastern Europe in spring 2006, Atmos. Chem. Phys., 7, 511–534, 2007, http://www.atmos-chem-phys.net/7/511/2007/. 26103

Tarasick, D., Moran, M., Thompson, A., Carey-Smith, T., Rochon, Y., Bouchet, V., Gong, W., Makar, P., Stroud, C., Ménard, S., Crevier, L., Cousineau, S., Pudykiewicz, J., Kallaur, A., Ménard, R., Robichaud, A., Cooper, O., Oltmans, S., Witte, J., Forbes, G., Johson, B., Merrill, J., Moody, J., Morris, G., Newchurch, M., Schmidlin, F., and Joseph, E.: Comparison of Canadian air quality forecast models with tropospheric ozone profile measurements above midlatitude North America during the IONS/ICARTT campaign: Evidence for stratospheric input0, J. Geophys. Res., 112, D12S22, doi:10.1029/2006JD007782., 2007. 26107

Taylor, K.: Summarizing multiple aspects of model performance in a single diagram, J. Geophys. Res., 107, 7183–7192, 2001. 26105

TF HTAP: Task Force on Hemispheric Transport of Air Pollution, Interim report, Air Pollution Studies No. 16, edited by : Keating, T. J. and Zuber, A., United Nations Economic Commission for Europe, New York, available at: www.htap.org, 2007. 26098, 26099, 26100

The Royal Society: Ground level ozone in the 21st century: future trends, impacts and policy implications, The Royal Society, Science Policy, London, RS Policy document 15/08 (Chair David Fowler), available at: www.royalsociety.org, 2008. 26101

Tong, D. and Mauzerall, D.: Spatial variability of summertime tropospheric ozone over the continental United States: Implications of an evaluation of the CMAQ model7, Atmos. Environ., 40, 3041–3056, 2006. 26107

Wild, O., Pochanart, P., and Akimoto, H.: Trans-Eurasian transport of ozone and its precursors, J. Geophys. Res., 109, D11302, doi:10.1029/2003JD004501, 2004. 26100, 26115

Zhang, L., Jacob, D., Kopacz, M., Henze, D., Singh, K., and Jaffe, D.: Mid-latitude tropospheric ozone columns from the MOZAIC program: climatology and interannual variability, Geophys. Res. Lett., 36, L11810, doi:10.1029/2009GL037950, 2009. 26100, 26117

Table 1. Models for which vertical profiles have been uploaded to TF HTAP server. Documentation of the models can be found at http://www.htap.org/ under the heading: Model Descriptions. Only the 7 first models (in bold) have uploaded vertical profiles for the SR20% scenarios.

Model	Resolution (lat long layers)	upper bound.	Institution	contact person HTAP
MOZARTGFDL 2[1]	1.88°×1.88°×28	0.66 hPa	GFDL, USA	Arlene Fiore
CAMCHEM 3311m13	2.5°×2.5°×30	2.5 hPa	NCAR, USA	Peter Hess
LMDz-INCA vSSz	2.5°×3.75°×19	3 hPa	CEA, France	Sophie Szopa
EMEP rv2.6[2]	1.0°×1.0°×20	100 hPa	met. no, Norway	Jan E. Jonson
FRSGC/UCI	2.81°×2.81°×37	0.1 hPa	Univ. Lancaster, UK	Oliver Wild
CAMCHEM 3514	2.5°×2.5°×30	2.5 hPa	NCAR, USA	Peter Hess
TM5-JRC-cy2-ipcc	1.0°×1.0°×25	0.48 hPa	JRC, Italy	Frank Dentener
UM CAM-v01[1]	3.75°×2.5°×19	4.6 hPa	Univ. Cambridge, UK	Guang Zeng
* MOZECH-v16	2.81°×2.81°×31	10 hPa	FZ Jülich, Germany	Martin Schultz
GEMAQ-v1p0	4.0°×4.0°×28	10 hPa	York Univ., Canada	Alexandru Lupu
GMI-v02f	2.5°×2.0°×42	0.01 hPa	NASA GSFC, USA	Bryan Duncan
CHASER v3.0	2.8°×2.8°×32	ca. 40 km	Nagoya Univ., Japan	Kengo Sudo

[1] No chemistry above tropopause level.
[2] Interpolated from 100×100 km^2 polar stereographic grid, N. Hemisphere only. No chemistry above approximately 14 000 m.
Prescribed O_2 and NO_y above 30 hPa.

ACPD
9, 26095–26142, 2009

Table 2. Measured and model calculated (see Table 1) ozone (ppb) for LT (900–700 hPa), MT (700–500 hPa) and UT (500–300 hPa) for the selected ozone sonde sites. corr. refer to the correlation between sonde measurements and models in the indicated height intervals. The numbers behind the site name refer to the number of soundings available in winter and spring respectively. Goose B. is short for Goose Bay.

	Winter (Jan, Feb)						Spring (Mar, Apr, May)					
	LT	corr.	MT	corr.	UT	corr.	LT	corr.	MT	corr.	UT	corr.
Goose B. (7, 10)	**38.1**		**46.1**		**73.8**		**50.8**		**60.4**		**84.1**	
MOZARTGFDL 2	36.0	0.510	46.4	0.406	72.5	−0.055	47.3	0.676	53.0	0.632	67.2	0.732
CAMCHEM 3311m13	45.9	0.151	53.2	0.505	75.5	0.561	54.2	0.854	60.9	0.929	75.8	0.725
LMDz-INCA vSSz	41.7	−0.620	46.9	0.538	56.9	−0.076	49.8	0.620	57.7	0.337	68.4	0.297
EMEP rv2.6	38.9	0.537	50.2	0.039	72.9	0.264	42.0	0.785	48.5	0.650	56.6	0.713
FRSGC/UCI	41.7	0.180	47.0	0.353	53.8	−0.609	52.4	0.199	60.3	0.478	69.6	0.449
CAMCHEM-3515	44.5	0.041	51.8	0.500	74.6	0.562	52.5	0.852	58.4	0.943	73.8	0.738
TM5	37.0	0.873	45.6	0.109	50.8	−0.626	48.3	0.567	57.7	0.502	66.8	0.334
UM-CAM-v01	35.3	0.306	39.8	0.883	45.8	−0.139	45.8	0.407	57.8	0.732	70.9	0.214
MOZECH-c16	39.2	0.674	48.1	0.676	53.8	−0.475	47.7	0.789	53.3	0.307	62.4	0.170
GEMAQ-v1p0	36.2	0.370	42.8	0.745	63.2	0.473	49.9	0.792	58.6	0.606	79.8	0.657
GMI-v02f	43.7	0.475	53.4	−0.204	64.8	−0.108	57.7	0.434	65.1	0.461	78.6	0.373
CHASER-v03	32.4	0.258	44.2	0.850	69.6	0.682	45.5	0.864	57.4	0.592	80.7	0.628
Uccle (26, 33)	**42.7**		**49.0**		**55.4**		**50.2**		**59.2**		**75.2**	
MOZARTGFDL 2	41.5	0.315	48.0	0.532	57.9	0.543	45.3	0.559	51.2	0.291	64.4	0.653
CAMCHEM 3311m13	48.8	0.471	54.4	0.414	63.0	0.497	54.6	0.476	59.5	0.182	73.9	0.612
LMDz-INCA vSSz	41.9	0.259	50.8	0.010	59.7	−0.065	52.2	0.383	57.3	0.313	62.3	0.014
EMEP rv2.6	46.9	0.098	55.3	0.117	63.4	0.359	48.7	0.559	48.2	0.458	56.8	0.628
FRSGC/UCI	46.1	0.246	49.9	0.171	54.0	−0.154	57.4	0.576	60.1	0.323	66.5	0.108
CAMCHEM-3515	47.5	0.468	53.1	0.418	61.8	0.508	52.9	0.486	57.2	0.109	72.0	0.603
TM5	42.8	0.260	47.3	0.171	54.4	−0.244	52.2	0.557	56.8	0.537	63.6	0.300
UM-CAM-v01	39.4	−0.088	42.7	−0.063	46.4	0.270	55.4	0.250	61.4	0.090	69.0	0.107
MOZECH-c16	45.0	0.436	51.8	0.126	57.0	−0.413	47.5	0.683	53.2	0.259	61.3	0.008
CEMAQ-v1p0	37.3	0.486	46.3	0.308	63.5	0.065	50.5	0.559	57.8	0.225	78.2	0.396
GMI-v02f	50.5	0.275	58.3	0.324	66.5	−0.149	56.4	0.538	64.6	0.319	74.8	0.544
CHASER-v03	39.7	0.357	48.0	0.135	64.7	0.180	49.3	0.500	56.0	0.339	81.1	0.127

Table 2. Continued.

	Winter (Jan, Feb)						Spring (Mar, Apr, May)					
	LT	corr.	MT	corr.	UT	corr.	LT	corr.	MT	corr.	UT	corr.
Tr. H. (8, 19)	**46.7**		**52.3**		**59.7**		**51.0**		**54.6**		**68.9**	
MOZARTGFDL 2	45.0	0.605	50.9	0.090	65.1	0.186	43.8	0.126	50.8	0.526	61.4	0.859
CAMCHEM 3311m13	51.4	0.800	56.2	0.340	63.1	−0.049	51.5	0.225	55.8	0.607	65.7	0.719
LMDz-INCA vSSz	49.6	0.846	57.5	0.354	65.8	−0.011	50.0	0.216	59.8	0.442	65.5	0.369
EMEP rv2.6	47.7	0.100	49.9	−0.177	74.5	−0.576	42.1	−0.372	43.9	0.656	59.2	0.373
FRSGC/UCI	49.0	0.791	51.1	0.452	58.0	0.018	49.5	0.028	53.1	0.075	57.0	0.333
CAMCHEM-3515	50.3	0.783	55.1	0.339	61.9	−0.004	49.1	0.137	54.1	0.610	64.0	0.728
TM5	47.0	0.769	52.4	0.289	62.7	−0.081	47.1	0.048	53.4	0.689	63.4	0.371
UM-CAM-v01	41.7	0.825	45.3	0.164	48.9	0.283	48.6	0.348	57.8	0.500	64.5	0.048
MOZECH-c16	48.5	0.851	55.0	0.032	63.7	−0.143	47.8	−0.039	54.0	0.260	62.2	0.368
CEMAQ-v1p0	42.1	0.855	53.7	−0.069	75.8	0.064	48.4	0.411	61.8	0.541	81.4	0.528
GMI-v02f	56.9	0.945	65.6	0.372	70.8	0.036	59.7	−0.042	66.3	0.227	77.4	0.522
CHASER-v03	44.8	0.922	54.7	0.222	74.1	0.069	46.6	0.073	56.3	0.405	79.4	0.727
Yakutsk (15, 5)	**38.4**		**43.6**		**57.0**		**46.8**		**56.6**		**81.8**	
MOZARTGFDL 2	39.8	0.320	48.8	0.226	71.5	−0.059	52.7	−0.084	55.3	−0.288	89.8	−0.189
CAMCHEM 3311m13	46.3	0.271	54.2	0.324	76.0	−0.004	55.5	−0.343	61.4	−0.242	72.8	−0.227
LMDz-INCA vSSz	41.9	0.201	46.0	0.166	56.8	0.252	54.9	−0.021	59.8	−0.491	64.4	0.198
EMEP rv2.6	41.4	−0.282	52.0	−0.714	63.0	−0.358	49.8	−0.447	46.1	−0.300	50.4	−0.020
FRSGC/UCI	44.6	0.246	48.3	0.123	54.5	0.181	62.2	−0.054	65.3	−0.404	66.9	−0.193
CAMCHEM-3515	45.1	0.251	52.9	0.321	75.2	0.003	53.6	−0.419	59.3	−0.263	70.9	−0.157
TM5	36.6	0.229	44.1	0.069	53.6	0.167	53.4	−0.101	62.3	−0.501	66.7	−0.045
UM-CAM-v01	38.3	0.504	44.9	0.302	50.9	−0.098	49.8	0.312	55.8	0.595	61.5	−0.325
MOZECH-c16	40.3	0.248	48.3	0.137	55.7	0.303	53.3	−0.020	55.4	−0.648	60.0	0.385
CEMAQ-v1p0	39.2	0.397	44.8	0.430	64.8	0.316	53.2	−0.097	59.0	−0.123	75.8	0.018
GMI-v02f	46.5	0.272	54.3	0.157	71.5	0.252	60.1	−0.175	66.0	−0.830	73.8	0.055
CHASER-v03	34.4	0.246	46.0	0.238	78.2	0.383	49.0	−0.283	56.6	−0.223	76.3	−0.636

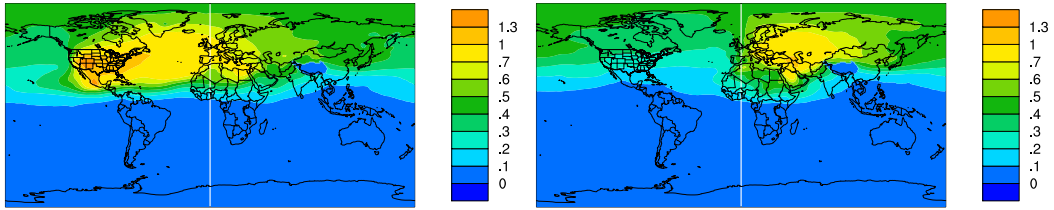

a) SRref − SR20%NA

b) SRref − SR20%EU

c) SRref − SR20%EA

Fig. 1. Effects of emission reductions in North America **(a)**, Europe **(b)** and East Asia **(c)** on ozone (ppb) in the lower free troposphere (750 hPa) averaged over one year calculated with the model ensemble of the first 7 models listed in Table 1. The zero contribution over the Himalayas is caused by the 750 hPa surface being below the surface here.

ACPD
9, 26095–26142, 2009

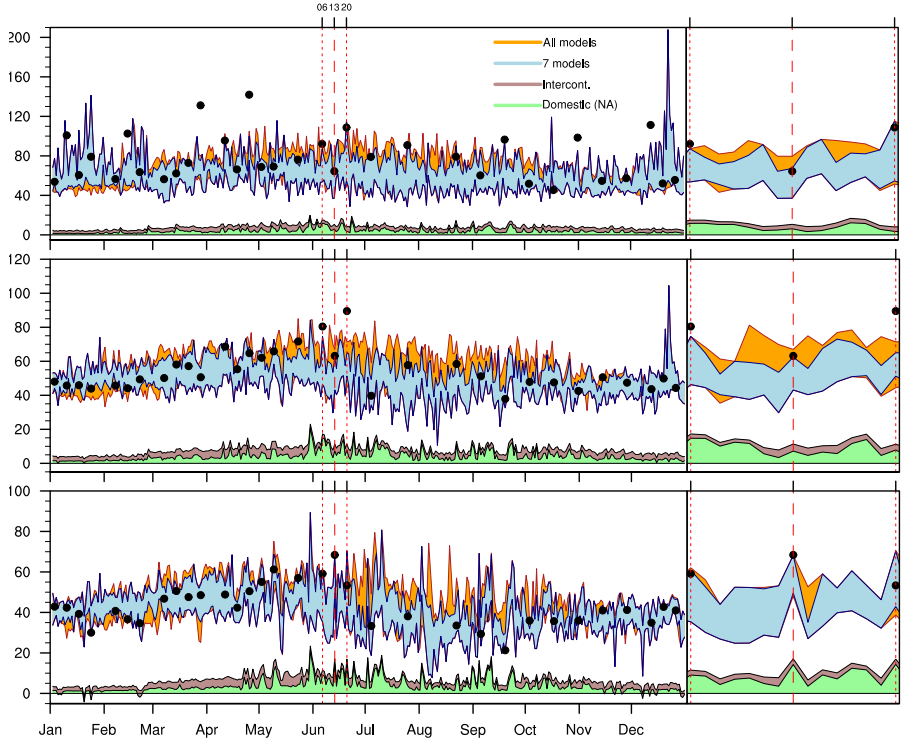

Fig. 2. Daily range of noon ozone levels in ppb for Goose Bay in the UT (top panel), MT (middle panel) and LT (lower panel). The focused panels on the right hand side are centred around 13 June. episode, highlighted in Sect. 4.2 and bounded by red lines in the figure. The range for the first seven models listed in Table 1 are shown in blue. The additional range, including all models in Table 1, are shown in orange. Ozone measurements from ozone sondes are marked as black dots. The model mean stacked contributions (multipl. by 5) from domestic (NA) and intercontinental (EU, EA and SA) are also shown.

ACPD
9, 26095–26142, 2009

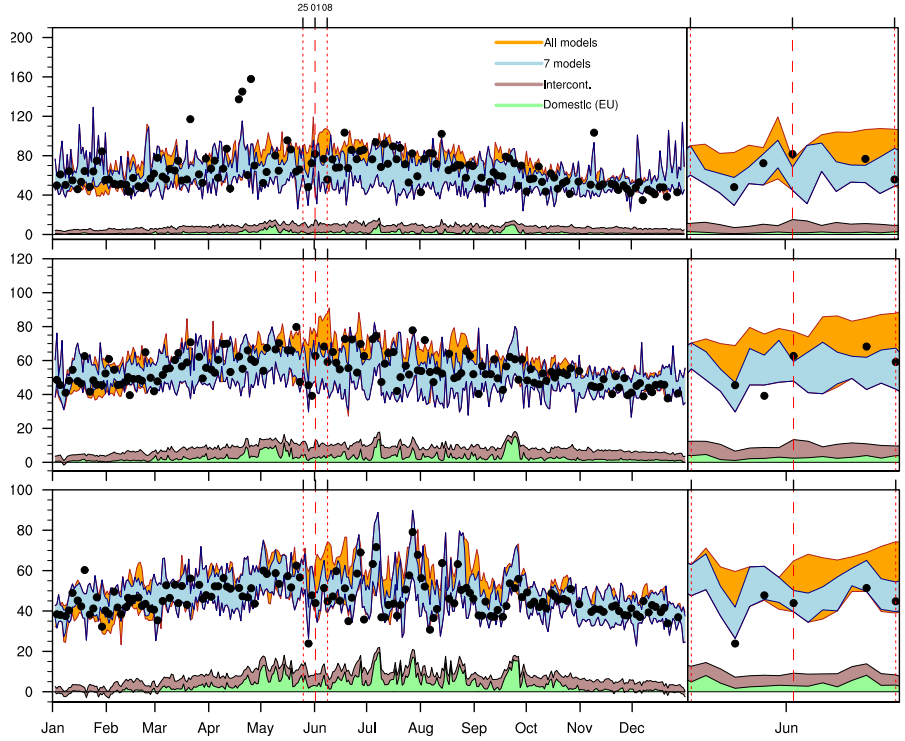

Fig. 3. Daily range of calculated ozone in UT, MT and LT and stacked contributions from NA, EU, EA and SA at Uccle. The focused panels on the right hand side are centred around 1 June. episode, highlighted in Sect. 4.3 and bounded by red lines in the figure. The range for the first seven models listed in Table 1 are shown in blue. The additional range, including all models in Table 1, are shown in orange. Ozone measurements from ozone sondes are marked as black dots. The model mean stacked contributions (multipl. by 5) from domestic (EU) and intercontinental (NA, EA and SA) are also shown.

ACPD
9, 26095–26142, 2009

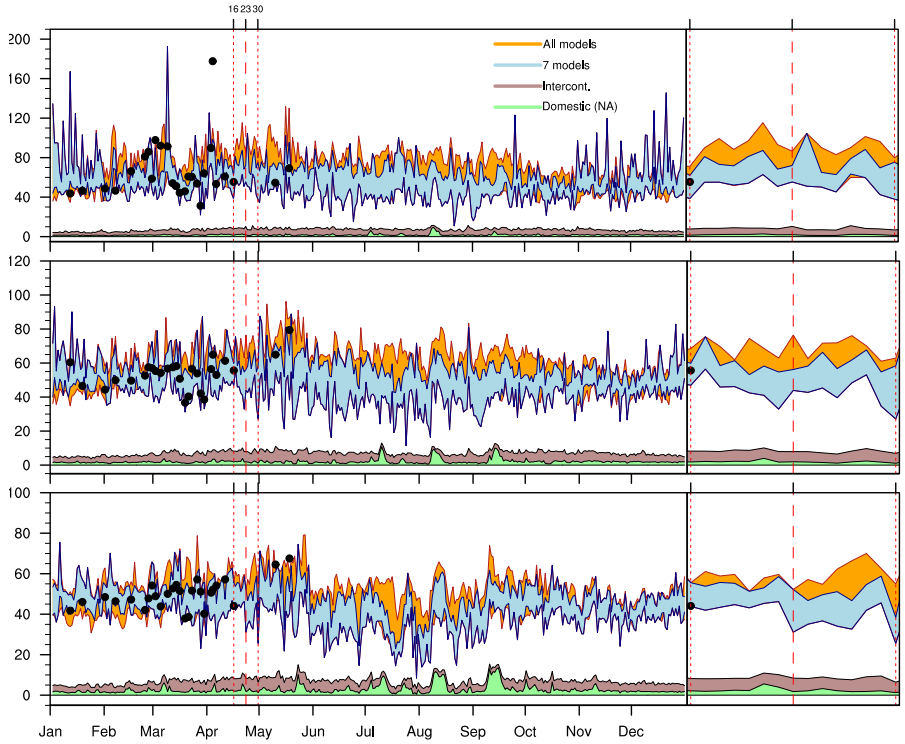

Fig. 4. Daily range of calculated ozone in UT, MT and LT and stacked contributions from NA, EU, EA and SA at Trinidad Head. The focused panels on the right hand side are centred around 23 April. episode, highlighted in Sect. 4.4 and bounded by red lines in the figure. The range for the first seven models listed in Table 1 are shown in blue. The additional range, including all models in Table 1, are shown in orange. Ozone measurements from ozone sondes are marked as black dots. The model mean stacked contributions (multipl. by 5) from domestic (NA) and intercontinental (EU, EA and SA) are also shown.

ACPD
9, 26095–26142, 2009

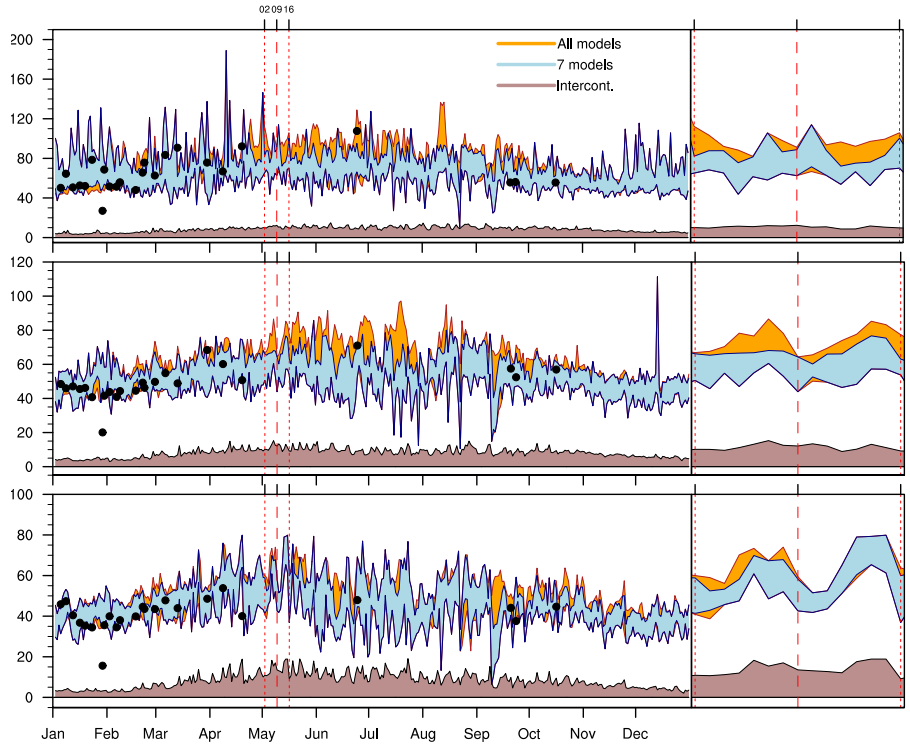

Fig. 5. Daily range of calculated ozone in UT, MT and LT and stacked contributions from NA, EU, EA and SA at Yakutsk. The focused panels on the right hand side are centred around 9 May. episode, highlighted in Sect. 4.5 and bounded by red lines in the figure. The range for the first seven models listed in Table 1 are shown in blue. The additional range, including all models in Table 1, are shown in orange. Ozone measurements from ozone sondes are marked as black dots. The model mean stacked contributions (multipl. by 5) from intercontinental (all regions, NA, EU, EA and SA) are also shown.

ACPD
9, 26095–26142, 2009

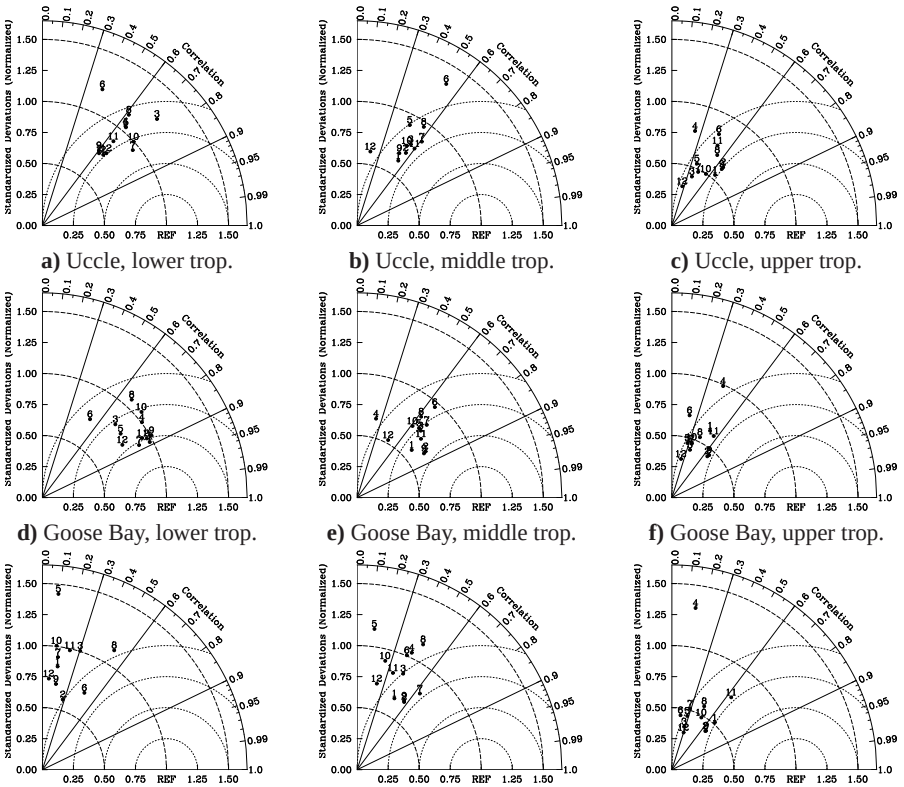

a) Uccle, lower trop. **b)** Uccle, middle trop. **c)** Uccle, upper trop.

d) Goose Bay, lower trop. **e)** Goose Bay, middle trop. **f)** Goose Bay, upper trop.

g) Trinidad Head, lower trop. **h)** Trinidad Head, middle trop. **i)** Trinidad Head, upper trop.

Fig. 6. Taylor diagrams showing correlations, normalised standard deviations (proportional to the radial distance from the origin) and RMS errors (proportional to the point on the x-axis identified as "REF") for the comparison of ozone soundings and calculated vertical profiles for the 12 models listed in Table 1.

ACPD
9, 26095–26142, 2009

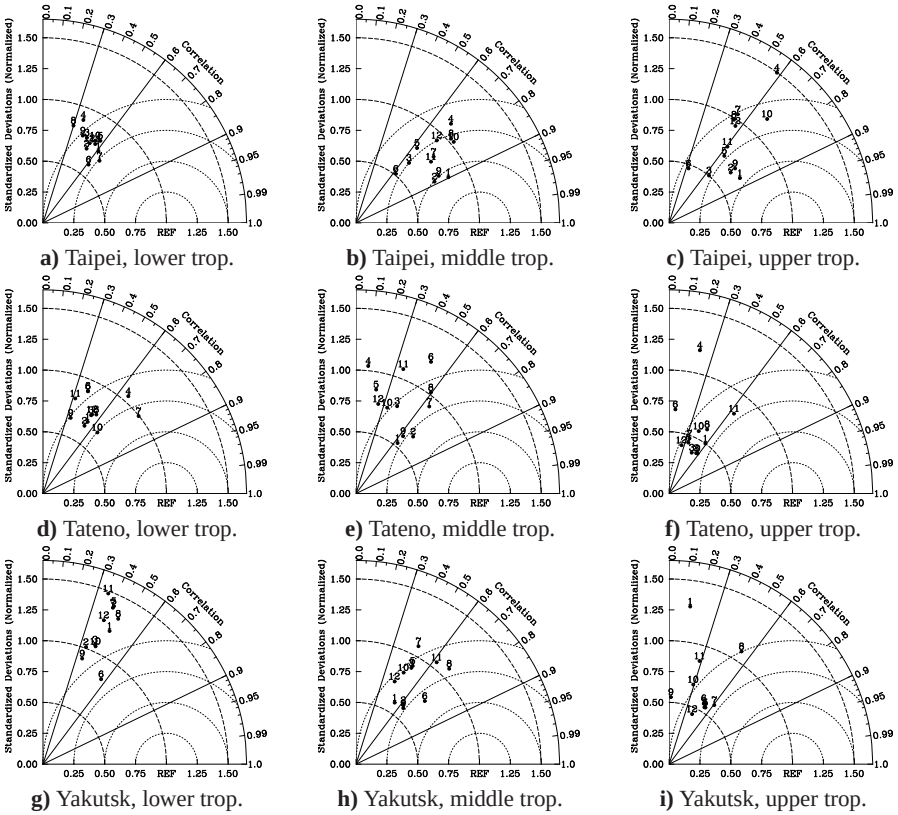

Fig. 7. Taylor diagrams showing correlations, normalised standard deviations (proportional to the radial distance from the origin) and RMS errors (proportional to the point on the x-axis identified as "REF") for the comparison of ozone soundings and calculated vertical profiles for the 12 models listed in Table 1.

ACPD
9, 26095–26142, 2009

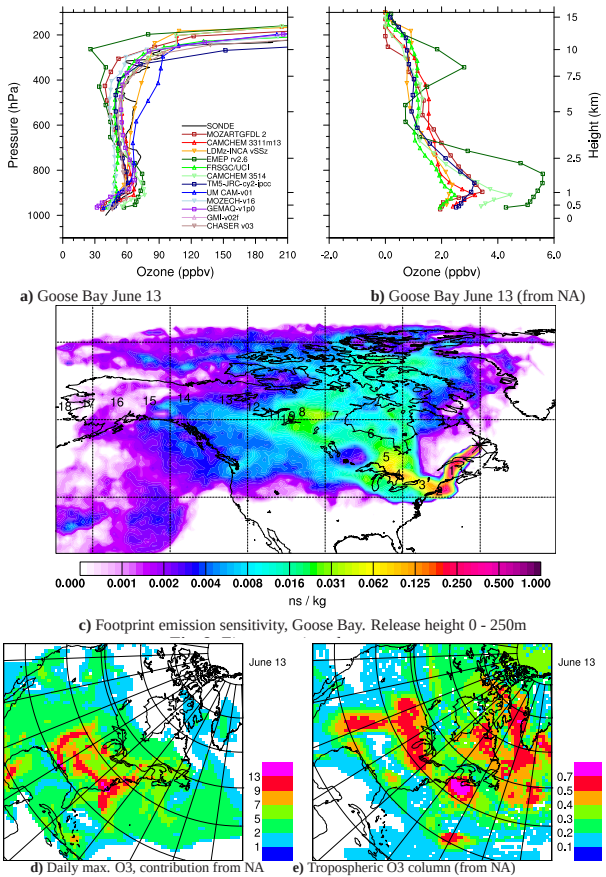

Fig. 8. All panels for 13 June, 12:00 UTC. **(a)** Ozone sounding and calculated vertical profiles for the 12 models listed in Table 1 in ppb. **(b)** Calculated difference SRref–SR20%NA in ppb for the 7 models, showing the effect of a 20% reduction of North American emissions. **(c)** FLEXPART footprint emission sensitivity for Goose Bay for the 0–250 m layer. The asterisk marks the position of the ozone sonde site. **(d)** Difference (SRref–SR20%NA) in daily maximum surface ozone in ppb calculated with the EMEP model. **(e)** Difference (SRref–SR20%NA) in tropospheric ozone column (DU) calculated with the EMEP model.

ACPD
9, 26095–26142, 2009

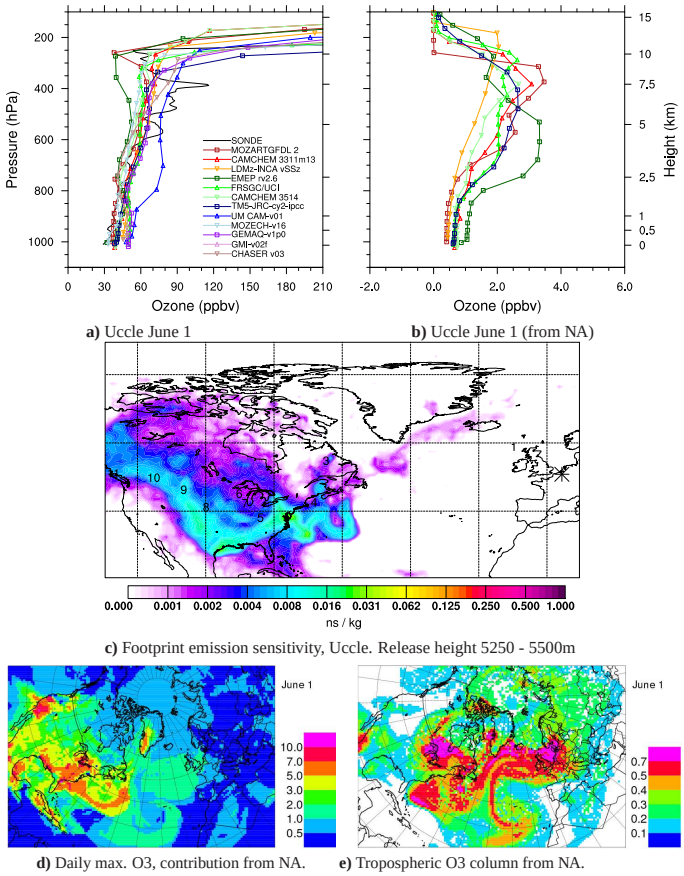

Fig. 9. All panels for 1 June, 12:00 UTC. **(a)** Ozone sounding and calculated vertical profiles in ppb for the 12 models listed in Table 1. **(b)** Calculated difference SRref–SR20%NA in ppb for the 7 models, showing the effect of a 20% reduction of North American emissions. **(c)** Footprint emission sensitivity (release height 5250–5500 m) from Uccle. The asterisk marks the position of the ozone sonde site. **(d)** Difference (SRref–SR20%NA) in daily maximum surface ozone in ppb calculated with the EMEP model. **(e)** Difference (SRref–SR20%NA) in tropospheric ozone column (DU) calculated with the EMEP model.

ACPD
9, 26095–26142, 2009

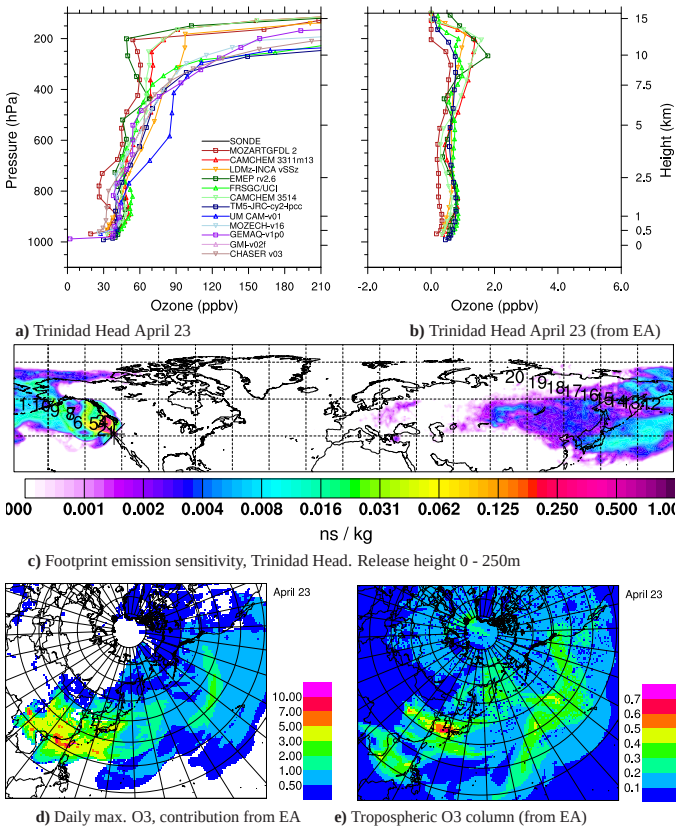

Fig. 10. All panels for 23 April, 12:00 UTC. **(a)** Ozone sounding and calculated vertical profiles in ppb for the 12 models listed in Table 1. **(b)** Calculated difference SRref–SR20%EA in ppb for the 7 models, showing the effect of a 20% reduction of East Asian emissions. **(c)** Footprint emission sensitivity (release height 0–250 m) from Trinidad Head. The asterisk marks the position of the ozone sonde site. **(d)** Difference (SRref–SR20%EA) in daily maximum surface ozone in ppb calculated with the EMEP model. **(e)** Difference (SRref–SR20%EA) in tropospheric ozone column (DU) calculated with the EMEP model.

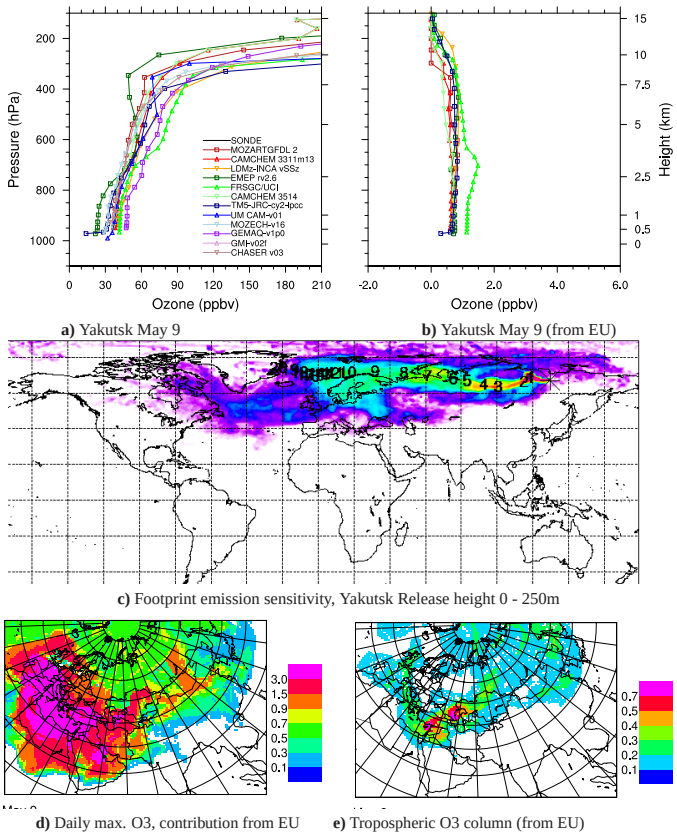

Fig. 11. All panels for 9 May, 12:00 UTC. **(a)** Ozone sounding and calculated vertical profiles in ppb for the 12 models listed in Table 1. **(b)** Calculated difference SRref–SR20%EU in ppb for the 7 models, showing the effect of a 20% reduction of European emissions. **(c)** Footprint emission sensitivity (release height 0–250 m) from Yakutsk. The asterisk marks the position of the ozone sonde site. **(d)** Difference (SRref–SR20%EU) in daily maximum surface ozone in ppb calculated with the EMEP model. **(e)** Difference (SRref–SR20%EU) in tropospheric ozone column (DU) calculated with the EMEP model.

ACPD
9, 26095–26142, 2009

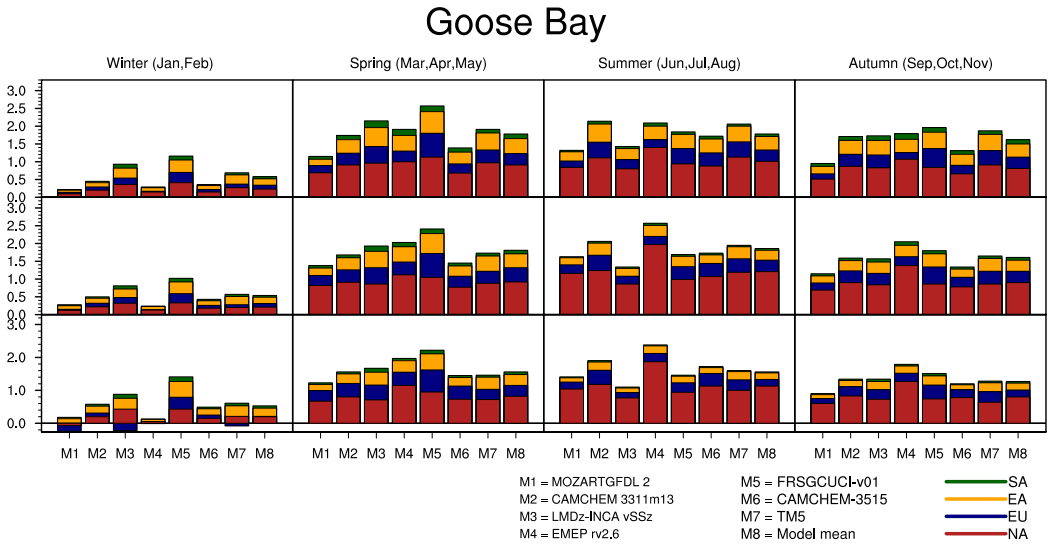

Fig. 12. Effects above Goose Bay on O_3 (ppb) of 20% reductions in emissions in the four source regions in winter, spring, summer and autumn calculated with the seven first models (and the model mean) listed in Table 1 (see legend above). Results are aggregated to LT (900–700 hPa), MT (700–500 hPa) and UT (500–300 hPa).

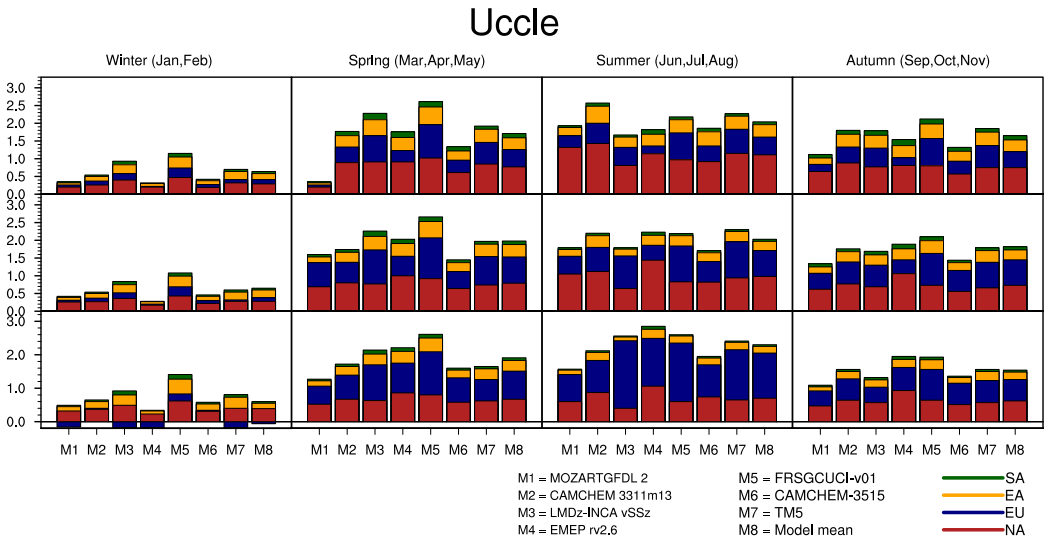

Fig. 13. Effects above Uccle on O_3 (ppb) of 20% reductions in emissions in the four source regions in winter, spring, summer and autumn calculated with the seven first models (and the model mean) listed in Table 1 (see legend above). Results are aggregated to LT (900–700 hPa), MT (700–500 hPa) and UT (500–300 hPa).

ACPD
9, 26095–26142, 2009

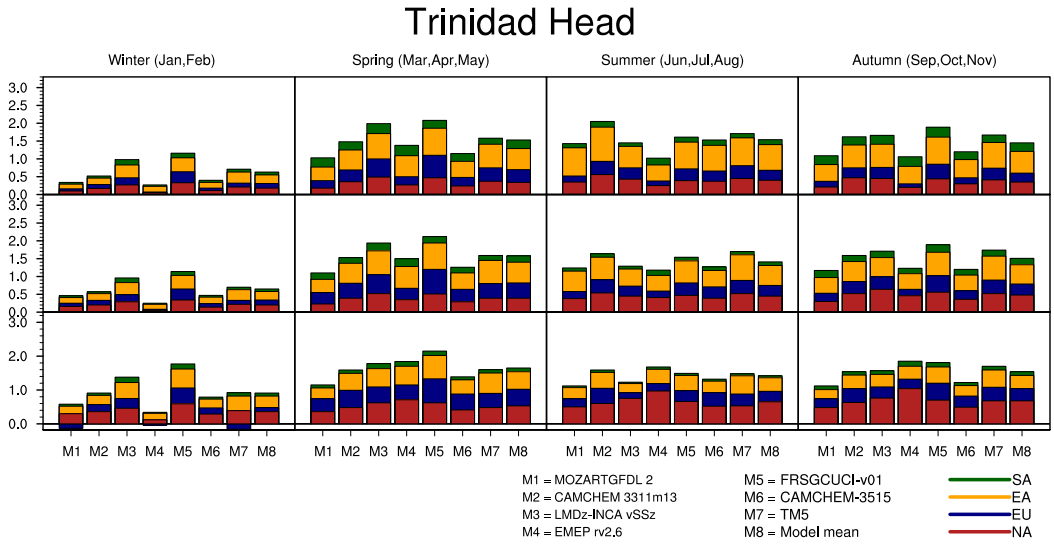

Fig. 14. Model calculated effect above Trinidad Head on O_3 (ppb) of 20% reductions in emissions in the four source regions in winter, spring, summer and autumn calculated with the seven first models (and the model mean) listed in Table 1 (see legend above). Results are aggregated to LT (900–700 hPa), MT (700–500 hPa) and UT (500–300 hPa).

ACPD
9, 26095–26142, 2009

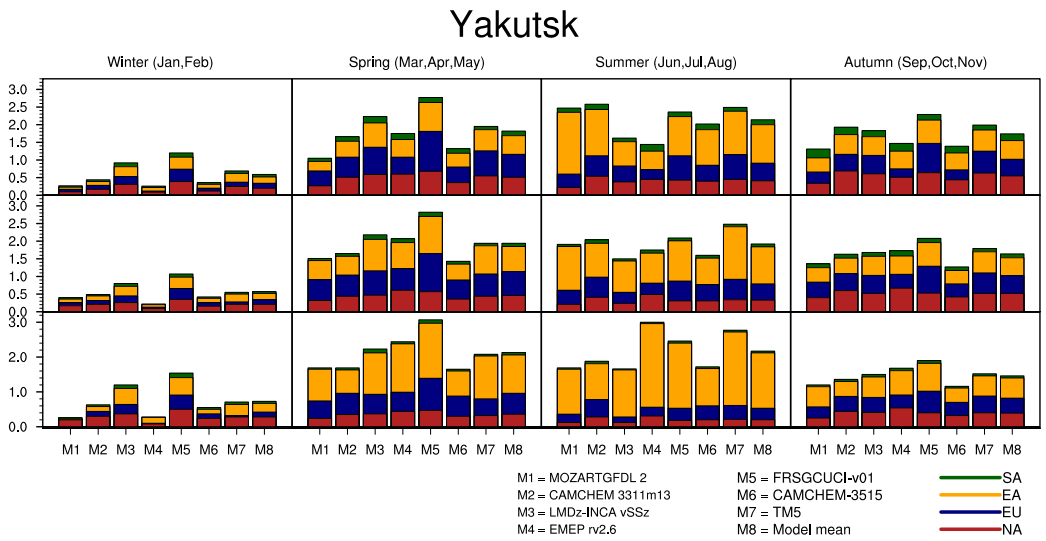

Fig. 15. Model calculated effect above Yakutsk on O_3 (ppb) of 20% reductions in emissions in the four source regions in winter, spring, summer and autumn calculated with the seven first models (and the model mean) listed in Table 1 (see legend above). Results are aggregated to LT (900–700 hPa), MT (700–500 hPa) and UT (500–300 hPa).

ACPD
9, 26095–26142, 2009